SANDIA REPORT

SAND2013-8289
Unlimited Release
Printed October 2013

Understanding and Controlling Low-Temperature Aging of Nanocrystalline Materials

Corbett C Battaile, Brad L Boyce, Justin G Brons, Stephen M Foiles, Khalid A Hattar, Elizabeth A Holm, Henry A Padilla, John A Sharon, Gregory B Thompson

Prepared by Corbett C Battaile
Sandia National Laboratories
Albuquerque, New Mexico 87185 and Livermore, California 94550

Sandia National Laboratories is a multi-program laboratory managed and operated by Sandia Corporation, a wholly owned subsidiary of Lockheed Martin Corporation, for the U.S. Department of Energy's National Nuclear Security Administration under contract DE-AC04-94AL85000.

Approved for public release; further dissemination unlimited.

Sandia National Laboratories

Issued by Sandia National Laboratories, operated for the United States Department of Energy by Sandia Corporation.

NOTICE: This report was prepared as an account of work sponsored by an agency of the United States Government. Neither the United States Government, nor any agency thereof, nor any of their employees, nor any of their contractors, subcontractors, or their employees, make any warranty, express or implied, or assume any legal liability or responsibility for the accuracy, completeness, or usefulness of any information, apparatus, product, or process disclosed, or represent that its use would not infringe privately owned rights. Reference herein to any specific commercial product, process, or service by trade name, trademark, manufacturer, or otherwise, does not necessarily constitute or imply its endorsement, recommendation, or favoring by the United States Government, any agency thereof, or any of their contractors or subcontractors. The views and opinions expressed herein do not necessarily state or reflect those of the United States Government, any agency thereof, or any of their contractors.

Printed in the United States of America. This report has been reproduced directly from the best available copy.

Available to DOE and DOE contractors from
U.S. Department of Energy
Office of Scientific and Technical Information
P.O. Box 62
Oak Ridge, TN 37831

Telephone: (865) 576-8401
Facsimile: (865) 576-5728
E-Mail: reports@adonis.osti.gov
Online ordering: http://www.osti.gov/bridge

Available to the public from
U.S. Department of Commerce
National Technical Information Service
5285 Port Royal Rd
Springfield, VA 22161

Telephone: (800) 553-6847
Facsimile: (703) 605-6900
E-Mail: orders@ntis.fedworld.gov
Online ordering: http://www.ntis.gov/help/ordermethods.asp?loc=7-4-0#online

SAND2013-8289
Unlimited Release
Printed October 2013

Understanding and Controlling Low-Temperature Aging of Nanocrystalline Materials

Corbett C Battaile, Brad L Boyce, Justin G Brons, Stephen M Foiles, Khalid A Hattar, Elizabeth A Holm, Henry A Padilla, John A Sharon, Gregory B Thompson

Abstract

Nanocrystalline copper films were created by both repetitive high-energy pulsed power, to produce material without internal nanotwins; and pulsed laser deposition, to produce nanotwins. Samples of these films were indented at ambient (298K) and cryogenic temperatures by immersion in liquid nitrogen (77K) and helium (4K). The indented samples were sectioned through the indented regions and imaged in a scanning electron microscope. Extensive grain growth was observed in the films that contained nanotwins and were indented cryogenically. The films that either lacked twins, or were indented under ambient conditions, were found to exhibit no substantial grain growth by visual inspection. Precession transmission electron microscopy was used to confirm these findings quantitatively, and show that $\Sigma 3$ and $\Sigma 7$ boundaries proliferate during grain growth, implying that these interface types play a key role in governing the extensive grain growth observed here. Molecular dynamics simulations of the motion of individual grain boundaries demonstrate that specific classes of boundaries - notably $\Sigma 3$ and $\Sigma 7$ - exhibit anti- or a-thermal migration, meaning that their mobilities either *increase* or do not change significantly with *decreasing* temperature. An in-situ cryogenic indentation capability was developed and implemented in a transmission electron microscope. Preliminary results do not show extensive cryogenic grain growth in indented copper films. This discrepancy could arise from the significant differences in configuration and loading of the specimen between the two approaches, and further research and development of this capability is needed.

Acknowledgments

The authors gratefully acknowledge contributions to this research from Michael T Marshall. The authors also wish to thank Robert Dickerson of Los Alamos National Laboratory for graciously supplying the Gatan 671 stage that enabled *in-situ* TEM experiments. This work was funded under LDRD Project Number 151344 and Title "Understanding and Controlling Low-Temperature Aging of Nanocrystalline Materials."

Contents

1 Introduction **7**

2 Cryogenic Micro-Indentation Experiments **9**

3 Mesoscale Simulations of Grain Growth **13**

4 Molecular Dynamics Simulations of Grain Boundary Mobilities **15**

5 Precession Transmission Electron Microscopy **25**

6 *In-Situ* Cryogenic Indentation Experiments in the TEM **29**

7 Conclusions **33**

References **34**

1. Introduction

Nanocrystalline metals offer exceptional properties, e.g. high strength, fatigue resistance, radiation hardness, and low friction. The greatest hurdle to applying these materials is the fact that their grain structures evolve at ambient temperatures, and recent evidence (see below) indicates that nanocrystalline metals can even evolve at cryogenic temperatures faster than they do at room temperature, as detailed in a recent review [1]. This can degrade properties and even accelerate failure. For example, large grains initiate fracture during fatigue of nanocrystalline nickel coatings, and coarsening of nanocrystalline copper lines in integrated circuits degrades their electronic properties. Still, low temperature grain growth remains a mystery. Microstructures are usually thought to be stable below about 40% of the melting temperature. This is because the grain boundary velocity, v, is the product of the driving pressure, p, and the boundary mobility, M, which decreases exponentially with temperature. Using parameters measured in aluminum, for example, the velocity of nanoscale grain boundaries is about forty micrometers per second at 70% of the melting temperature, but only about one femtometer per second at room temperature. According to these data, then, at cryogenic temperatures the boundaries shouldn't move perceptibly within the lifetime of the universe! So how can we explain, and ultimately control, ambient-temperature grain growth in nanocrystalline metals, so that we might develop strategies for mitigating the inherent instability of these otherwise advantageous materials?

The evolution of the internal structure of nanocrystalline metals is generally associated with a driving force that promote the motion of internal interfaces, e.g. elevated temperature or imparted stress. In the latter case, recent evidence [2] indicates that mechanical driving forces, imparted by indentation of thin films, can produce low-temperature grain growth in nanocrystalline copper at rates that exceed those of the comparable phenomenon observed at room temperature. This result is counter-intuitive, since grain boundary motion is (assumed to be) a thermally activated process, and should thus proceed more slowly at lower temperatures.

This report outlines a combination of experiments and simulations that were conducted as part of an LDRD program in an attempt to unravel the mysteries of low-temperature nanostructure evolution in nanocrystalline metals. We used indentation experiments in both ambient and cryogenic environments to isolate the variables responsible for enabling low-temperature growth, and to ascertain the conditions, material characteristics, and ultimately the mechanisms underlying this phenomenon. We pursued several techniques, including high-throughput molecular dynamics, *in-situ* nanoindentation in the TEM, and precession TEM imaging, to characterize the types of grains and interfaces that are prone to low-temperature migration. This document contains a summary of the key findings from this investigation, and the reader is referred to the references in the subsequent text for further information and detail, where appropriate.

2. Cryogenic Micro-Indentation Experiments

In order to confirm the findings in Ref [2] and to map the response of nanocrystalline copper thin films under various conditions, we performed micro-indentation tests at several loads on films with and without internal nanotwins in environments of air (298K), liquid nitrogen (77K), and liquid helium (4K). Figure 2.2 contains TEM images of two of the films created using different deposition methods. After indentation, the films were allowed to warm to room temperature (if needed) and the microstructures underneath the indentation were imaged in a scanning electron microscope. Figures 2.3 and 2.4 show SEM images of cross-sections through indented films that were initially untwinned then indented in air (Fig 2.3), and twinned then indented in cryogenic conditions (Fig 2.4), respectively. The films deposited by repetitive high-energy pulsed power show no obvious signs of extensive grain growth during or after indentation in air, whereas the pulsed laser deposited films indented under cryogenic conditions show obvious signs of extensive grain growth in the indented region, perhaps more so in helium (Fig 2.4(b) and 2.4(c)) than nitrogen (Fig 2.4(a)). Table 2.1 contains a summary of the results from all conditions (i.e. temperature and indentation load) and films tested. An entry of "YES" indicates that extensive grain growth was observed after indentation under the specified conditions; "NO" indicates that no evidence of substantial grain growth was observed; and a question mark ("?") denotes conditions that were not tested. Table 2.1 clearly demonstrates that two elements are required for extensive grain growth to occur in nanocrystalline copper films during/after indentation: the presence of nanotwins in the structure, and cryogenic conditions during indentation. Further details regarding these experiments can be found in Ref [3].

Table 2.1. "Truth table" showing indentation conditions and material types under which extensive grain growth does and does not occur in nanocrystalline copper.

	RHEPP Cu (untwinned)			PLD Cu (untwinned)			PLD Cu (twinned)			
	9.5 g	21 g	55 g	9.5 g	21 g	55 g	9.5 g	21 g	55 g	
Air	?	NO	?	?	?	?	NO	NO	NO	Air
N_2	?	NO	NO	?	NO	?	YES	YES	YES	N_2
He	NO	?	NO	?	NO	NO	YES	YES	YES	He

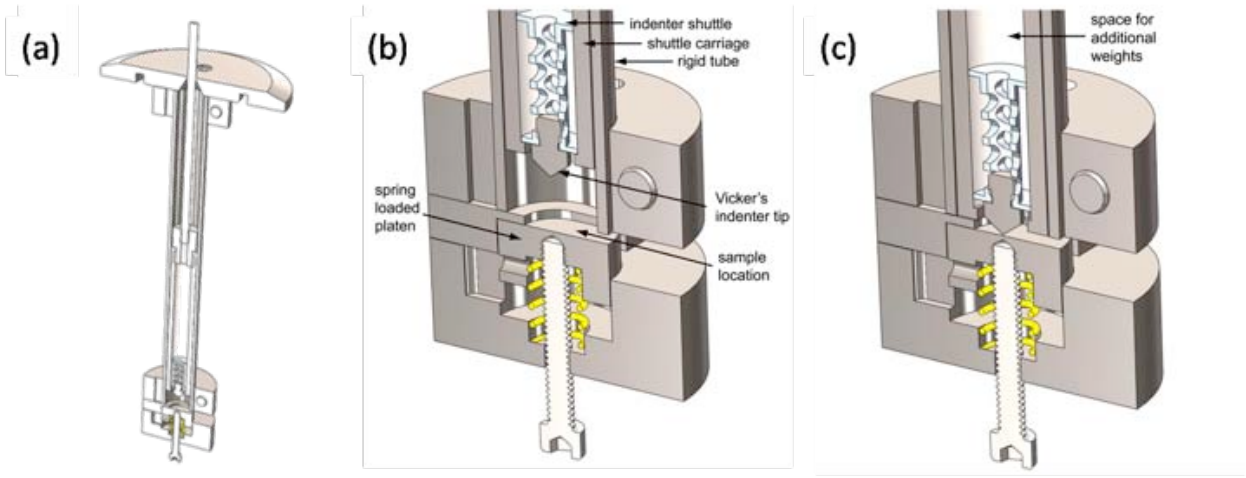

Figure 2.1. Cross-section schematic showing (a) components of the indenter apparatus as well as the (b) unloaded and (c) loaded positions. Cylindrical weights and sample are not shown.

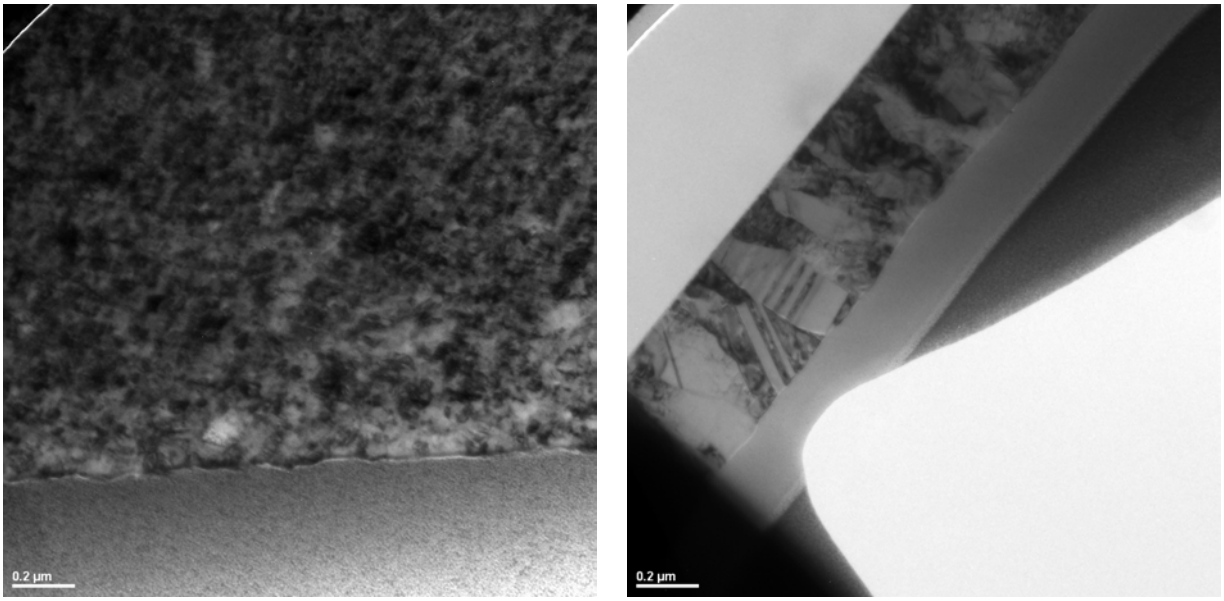

(a) (b)

Figure 2.2. Transmission electron micrographs of nanocrystalline copper films deposited by (a) repetitive high-energy pulsed power and (b) pulsed laser deposition.

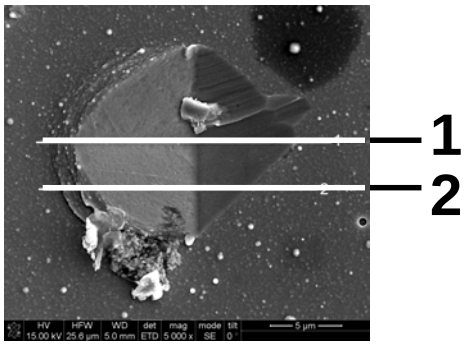

(a)

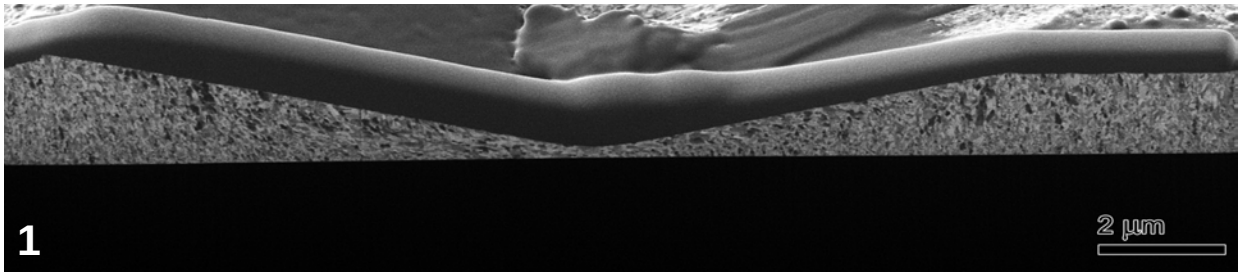

(b)

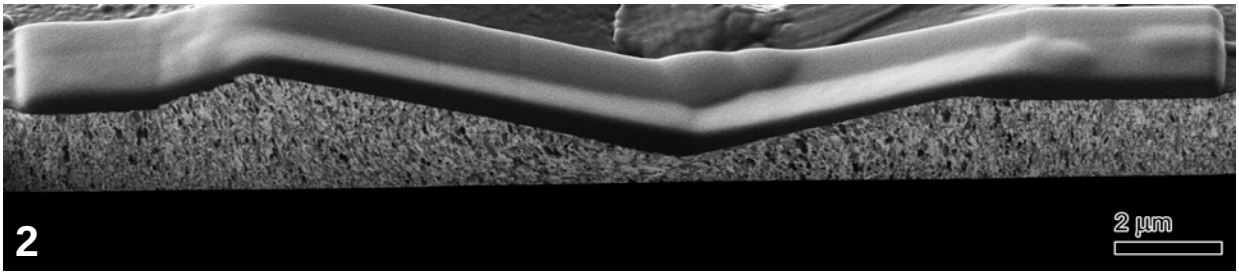

(c)

Figure 2.3. Cross-sectional scanning electron micrographs taken from (a) two locations through an indent, (b) one through the center and (c) another closer to the edge, in nanoycrystalline copper deposited by repetitive high-energy pulsed power.

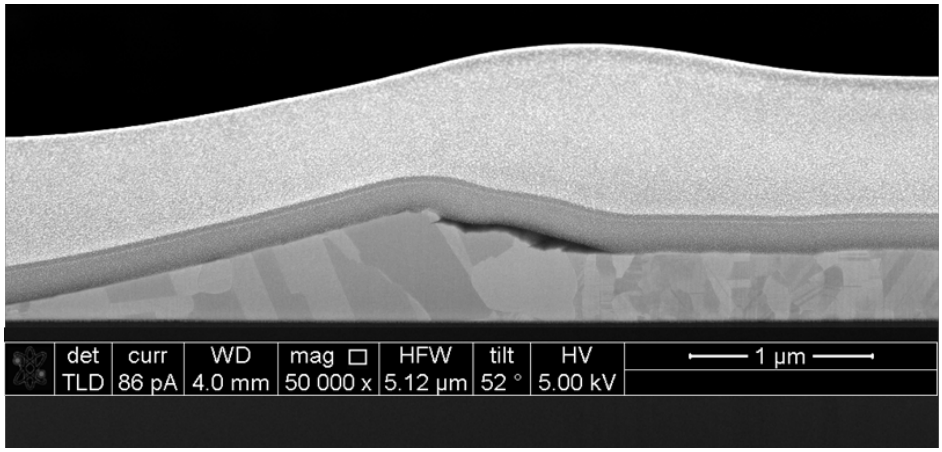

(a)

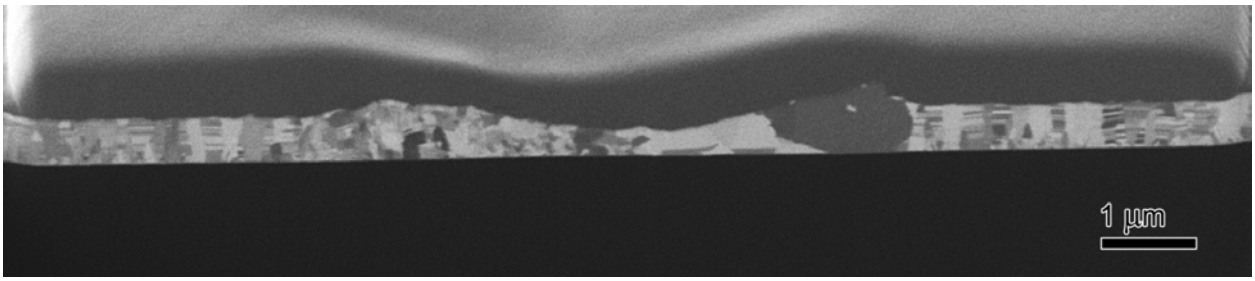

(b)

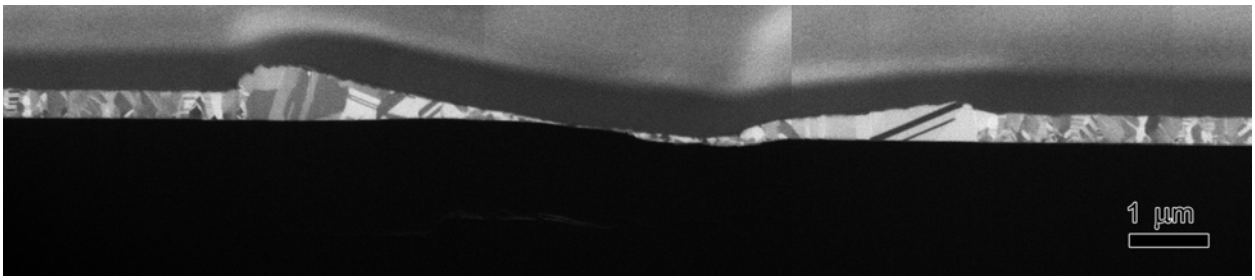

(c)

Figure 2.4. Cross-sectional scanning electron micrographs taken from nanoycrystalline copper deposited by pulsed laser and then indented in liquid (a) nitrogen and (b-c) helim.

3. Mesoscale Simulations of Grain Growth

While the results described above do not elucidate any mechanism for appreciable grain boundary mobility at low temperatures, we can still attempt to examine some aspects of the role of mechanical driving forces on grain growth at low temperatures. To do this, we turn to earlier mesoscale simulations of grain growth in deformed microstructures. We assume that the efficacy of dislocation motion, and this plastic deformation, is suppressed at very low temperatures, and thus the distinction between ambient and cryo conditions was simulated by the presence or absence of plastic deformation, representing ambient and cryo temperatures respectively. The grain growth process was modeled using a "sharp interface front tracking" approach, while deformation was simulated using the finite element method with a crystal plasticity constitutive model for dislocation plasticity in FCC metals. The two approaches were coupled sequentially, such that a polycrystalline microstructure was deformed in a finite element simulation to quantify the distribution of stresses and plastic strains throughout the model system, and then the mechanical state near each grain boundary was combined with the conventional curvature driving force to simulate the effects of stress and strain on the motion of the grain boundaries. Once the boundaries migrated a short distance, the modified geometry was supplied to the finite element simulation to re-compute the stresses and strains, and the procedure was repeated many times until sufficient evolution of the microstructure had occurred. Additional details of these simulations can be found in Ref [4].

The key result from this effort was that the suppression of plasticity (presumed to occur at very low temperatures) served to substantially elevate the rate of grain growth as compared to the case where plasticity is active (at ambient temperatures). This is because plasticity is inherently a stress relief mechanism. When that mechanism is suppressed, stresses are not relieved and can become elevated to levels well beyond those associated with the dissipative action of plastic flow. This is evidenced in Fig 3.1, where the ambient behavior corresponds to the dotted line, and the low-temperature to the solid.

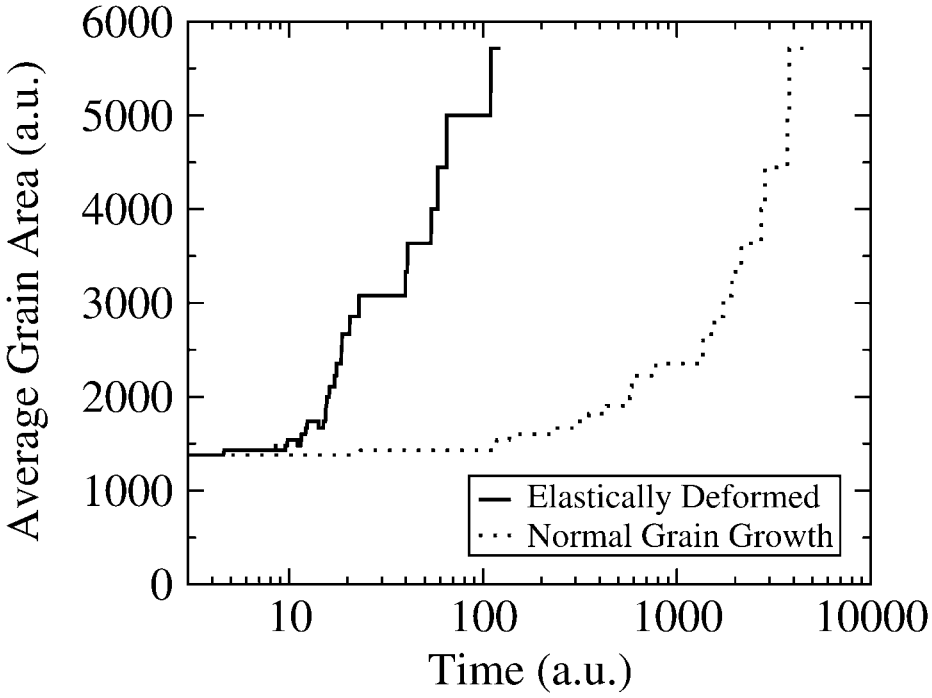

Figure 3.1. The acceleration of grain growth in a simulated copper polycrystal deformed in tension at very low temperature where predominantly elastic deformation only can occur (solid line), and at ambient temperature where elastic-plastic deformation occurs (dashed line).

4. Molecular Dynamics Simulations of Grain Boundary Mobilities

The results from the mesoscale grain growth simulations described in the previous chapter suggest a mechanism for the storage and consequent action of elevated mechanical driving forces that can lead to accelerated grain growth at low temperatures. However, the suppression of dislocation plasticity would presumably be accompanied by a concomitant suppression of the inherent mobility of the grain boundaries themselves, thus negating the action of the increased mechanical driving forces at low temperatures, and this phenomenon was not considered in the simulations described in Chapter 3. To examine this in more detail, we turn to molecular dynamics simulations of the mobilities of various types of grain boundaries as a function of decreasing temperature [5]. As shown in Fig 4.1, while most types of grain boundaries exhibit the expected thermal behavior, i.e. decreasing mobility with decreasing temperature, as significant population of grain boundaries - approximately 20% of the total - show athermal or antithermal behavior wherein their mobilities appear to either remain relatively unchanged or to actually *increase* with decreasing temperature.

Knowledge of the properties of grain boundaries is a fundamental input into the understanding of the evolution of the grain microstructure. Prior to this project, an extensive study of the energy and mobility of a catalogue of 388 grain boundaries in nickel was performed by Olmsted et al [6, 7]. The set of boundaries studied contained all coincident site lattice (CSL) [8] boundaries that could be created with periodic cells in the plane of the boundary with dimensions less than or equal to $7\ ^1/_2$ lattice constants. During this project, follow studies related to these simulations were performed. These studies concerning energy focused on the generalization of the results to other face centered cubic (FCC) metals, the validation of the results compared to experimental observations. In addition, the mobility results were examined in connection with the coupling of shear and normal motion of the boundaries and further examination of the temperature dependence of grain boundary mobility. The latter two studies are particularly relevant to the possibility of cryogenic grain growth.

The calculations of grain boundary energy have been validated by comparisons with recent experimental studies of the variation of grain boundary energy [9, 10] as part of collaborations with Carnegie Mellon Univeristy. Prior to this project, grain boundary energies computed for nickel were compared directly to relative energies obtained from an extensive numerical analysis of experimental triple junction angles [9]. This comparison was favorable for those boundaries for which there was substantial experimental data. It has been observed empirically that there is a strong correlation between the frequency with which grain boundaries occur and their energy. The relative area of different grain boundary ge-

ometries is referred to as the grain boundary character distribution (GBCD). The GBCD was determined a well-annealed sample of aluminum by the collaborators at Carnegie Mellon. Figure 4.2 shows a comparison of the experimentally observed GBCD measured by the logarithm of the boundary population plotted relative to the computed grain boundary energy [10] for those boundaries with a population greater than a random distribution. It is observed that there is a good correlation which validates the grain boundary energy calculations.

An important issue with regard to low-temperature grain growth is the role of local stresses on grain boundary motion. In particular, it has been observed that there can be a coupling between shear of a boundary and local motion of the boundary normal to the interface [8]. It has been argued recently that local stresses can in fact drive grain boundary motion and thus grain evolution [11, 12]. There has also been recent theoretical work on shear-coupling prompted by the work of Cahn and Mishin that shows a relationship between motion parallel and perpendicular to the boundary for tilt grain boundaries [13, 14].

In this project, the shear coupling mechanism has been addressed by Homer, Foiles, Holm, and Olmsted [15] via simulations of boundary motion for a wider range of grain boundaries and employing different simulation boundary conditions than used in prior studies These simulations employ a synthetic driving force [16] which induces boundary motion normal to the boundary plane while the earlier work of Cahn and Mishin [13, 14] impose a shear on the boundary and observe the motion normal to the boundary. Figure 4.3 illustrates the difference in the simulation boundary conditions of the bicrystal. In the work by Cahn and Mishin [13, 14], a shear force is applied parallel to the boundary so that the bicrystals will evolve from the initial state in Fig 4.3(a) to either Fig 4.3(b) or Fig 4.3(c). In the present work, a synthetic driving force is applied which induces motion normal to the boundary and the system will evolve from Fig 4.3(a) to either Fig 4.3(d) or Fig 4.3(e). Note that Fig 4.3(b) and Fig 4.3(d) are similar so in those cases the results from the present analysis and that of Cahn and Mishin [13, 14] can be directly compared. Another way that the comparison of the current work and Cahn's and Mishin's [13, 14] can be stated is that the latter sheared the boundary and asked if the boundary moves normal to the interface while in the present work, the boundary is moved normal to the interface and we ask if it shears.

Figure 4.4 presents the computed shear coupling factor for several symmetric tilt grain boundaries compared to predictions based on the dislocation content of the boundaries. The shear coupling factor is the ratio of the displacement of the boundary parallel to the interface to the displacement of the boundary normal to the interface. The results for the $\langle 100 \rangle$ symmetric tilt boundaries are consistent with those of Cahn and Mishin [13, 14], which indicates that the shear coupling mechanism does not depend on the nature of the driving force. The results for the other tilt boundaries are new. It is seen that shear coupling occurs for certain tilt boundaries that are comprised of compact dislocations as discussed in detail by Homer, Foiles, Holm, and Olmsted [15]. It is also noted that for those boundaries which undergo shear coupling consistent with a dislocation model, the coupling factor and the mobility are inversely related. Homer, Foiles, Holm, and Olmsted [15] also note that in some cases, the shear coupling behavior is temperature dependent.

In addition to the above studies of the mobility of planar grain boundaries in bi-crystal geometries, simulations of grain boundary networks were performed. In particular, Tucker and Foiles [17] simulated the evolution of the grain microstructure during the nano-indentation of a nano-crystalline sample. These simulations were performed at room temperature and for a range of indentation rates. In the simulations, the indenter is moved into the sample, held and then retracted. Figure 4.5 shows a cross-section of the simulation cell at three stages during the indentation process. The green shaded atoms are atoms with local FCC environments. The initial underformed grain structure shown in (a) is obtained by the annealing of a Voronoi tessellation grain structure with about half of the grain size. The anneal at 0.75 homologous temperature induced grain growth that resulted in the initial structure. The presence of grain growth even at these high-strain rates and at room temperature is evident in the final frame. An increase in the grain size for the grains near the indenter was also confirmed quantitatively in the analysis. The atoms shaded red have local hexagonal close-packed (HCP) environments and twin boundaries will thus show as single thickness red planes and stacking faults a double thickness red planes. Note that both twin boundary formation occurs as well as the passage of partial dislocations during the indentation.

The role of different deformation mechanisms was also determined by Tucker and Foiles [17] using micromechanics based metrics. This analysis shows that dislocation and twinning nucleation are important mechanisms that accompany grain growth that that these mechanisms are rate-dependent. Full dislocation slip is observed to be more prevalent that partial dislocation slip. During the period when the indenter is held in place and then retracted, it appears that grain boundary relaxation and local atomic rearrangements result in the emission of trailing partial dislocations from the grain boundary that eliminate stacking faults left behind during the indentation. Future work will correlate the relaxation mechanisms with the crystallography of the grain boundaries.

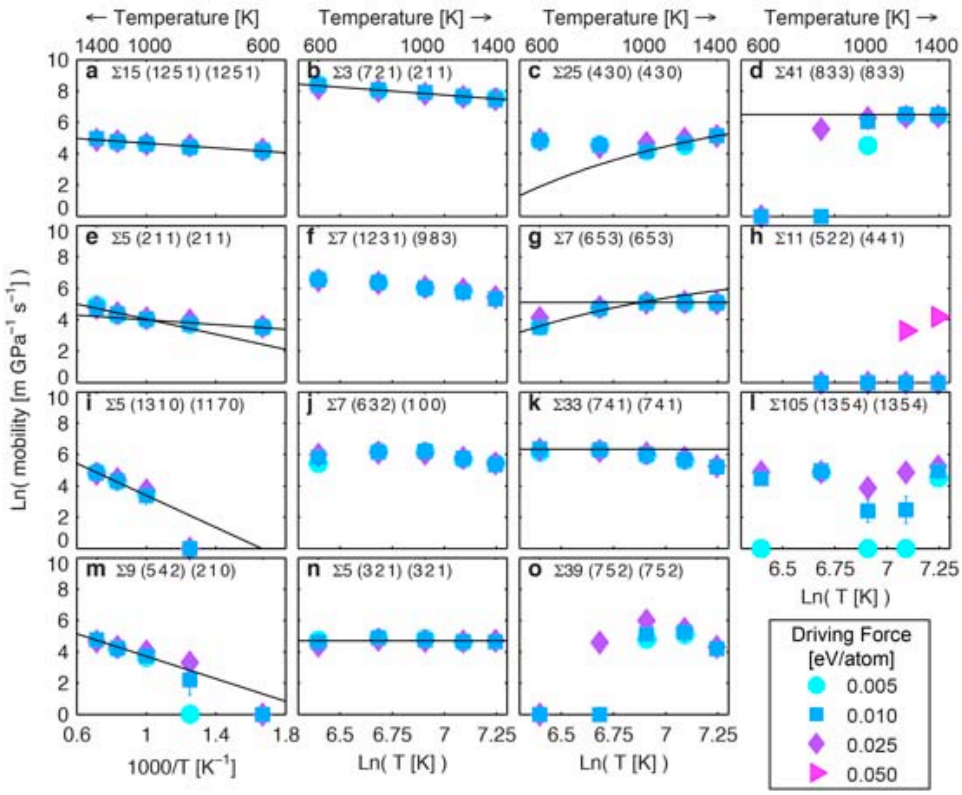

Figure 4.1. Illustration of all temperature-dependent mobility trends described in the taxonomy of Table 4.1. Note that the left column shows temperature in Arrhenius coordinates, while the others plot temperature logarithmically. The absolute temperature is shown above the plots. Trends illustrated are (a) thermally activated, (b) thermally damped, (c) thermally damped transitioning to thermally activated, (d) immobile transitioning to athermal, (e) thermally activated with two activation energies, (f) antithermal, (g) thermally activated transitioning to athermal, (h) immobile, (i) thermally activated with roughening, (j) antithermal with a maximum mobility, (k) athermal transitioning to antithermal, (l) unclassified unique temperature dependence, (m) thermally activated with dynamic roughening, (n) athermal, and (o) immobile transitioning to antithermal.

Table 4.1. Taxonomy of grain boundary motion trends. f_o indicates the number of boundaries observed to follow a given trend. (A total of 388 boundaries were analyzed.) The rightmost column indicates the mobility plot in Fig 4.1 that illustrates that particular behavior.

#	Trend	Description	f_o	Fig 4.1
		Thermally activated grain boundary motion		
1	Thermally activated	Constant activation energy.	11	(a)
2	Thermally activated, two activation energies	Change in activation energy at a distinct temperature. The higher activation energy always occurs in the higher temperature .	10	(e)
3	Thermally activated, roughening	Thermally activated above roughening temperature T_r; immobile on the MD time scale below T_r. Mobility is not driving-force dependent.	38	(i)
4	Thermally activated, dynamic roughening	As in #3 but near T_r the mobility is driving-force dependent; a high driving force can induce thermally activated motion below T_r.	162	(m)
		Non-thermally activated grain boundary motion		
5	Thermally damped	Mobility inversely proportional to temperature.	25	(b)
6	Antithermal	Mobility decreases as temperature increases; mobility is concave in temperature with maximum mobility at the minimum temperature.	26	(f)
7	Antithermal with mobility maximum	As in #6 but with maximum mobility at an intermediate temperature.	7	(j)
8	Athermal	Constant mobility over full range of temperature.	21	(n)
		Mixed-motion modes		
9	Antithermal - thermally activated	Antithermal at low temperature, transitioning to thermally activated at high temperature.	11	(c)
10	Thermally activated - athermal	Thermally activated at low temperature, saturating to a constant mobility at high temperature.	7	(g)
11	Athermal - antithermal	Antithermal at high temperature, saturating to a constant, athermal mobility at low temperature.	19	(k)
12	Immobile - antithermal	As in #3 but antithermal motion above T_r.	13	(o)
13	Immobile - athermal	As in #3 but athermal motion above T_r.	2	(d)
		Unclassifiable mechanisms		
14	Immobile	Immobile over the full temperature range.	25	(h)
15	Unique temperature dependence	Display a variety of temperature dependence not consistent with any other mechanism(s).	11	(l)

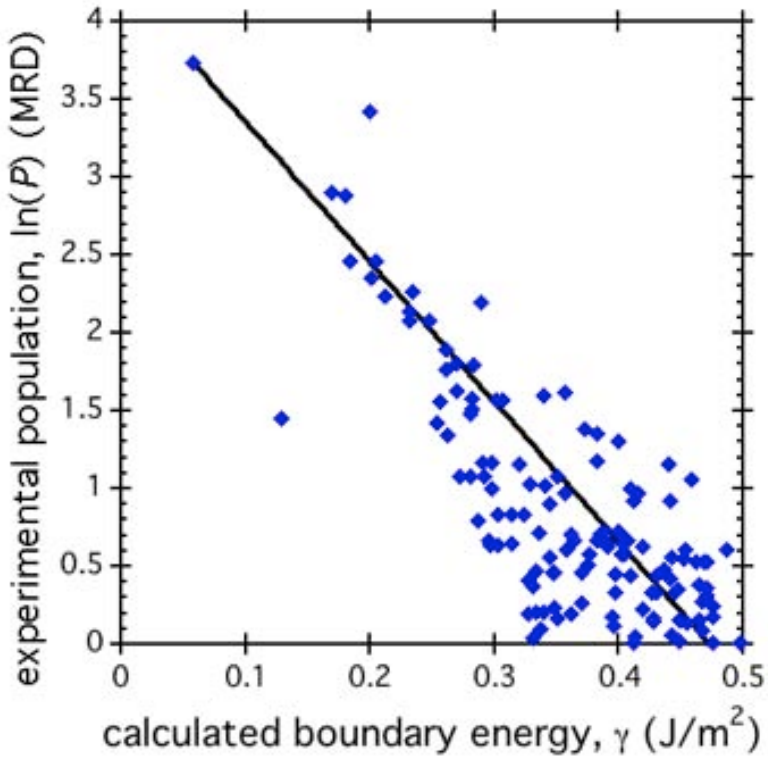

Figure 4.2. The relationship between experimental grain boundary character distribution (GBCD) and calculated grain boundary energy for aluminum for boundaries with high boundary population [10].

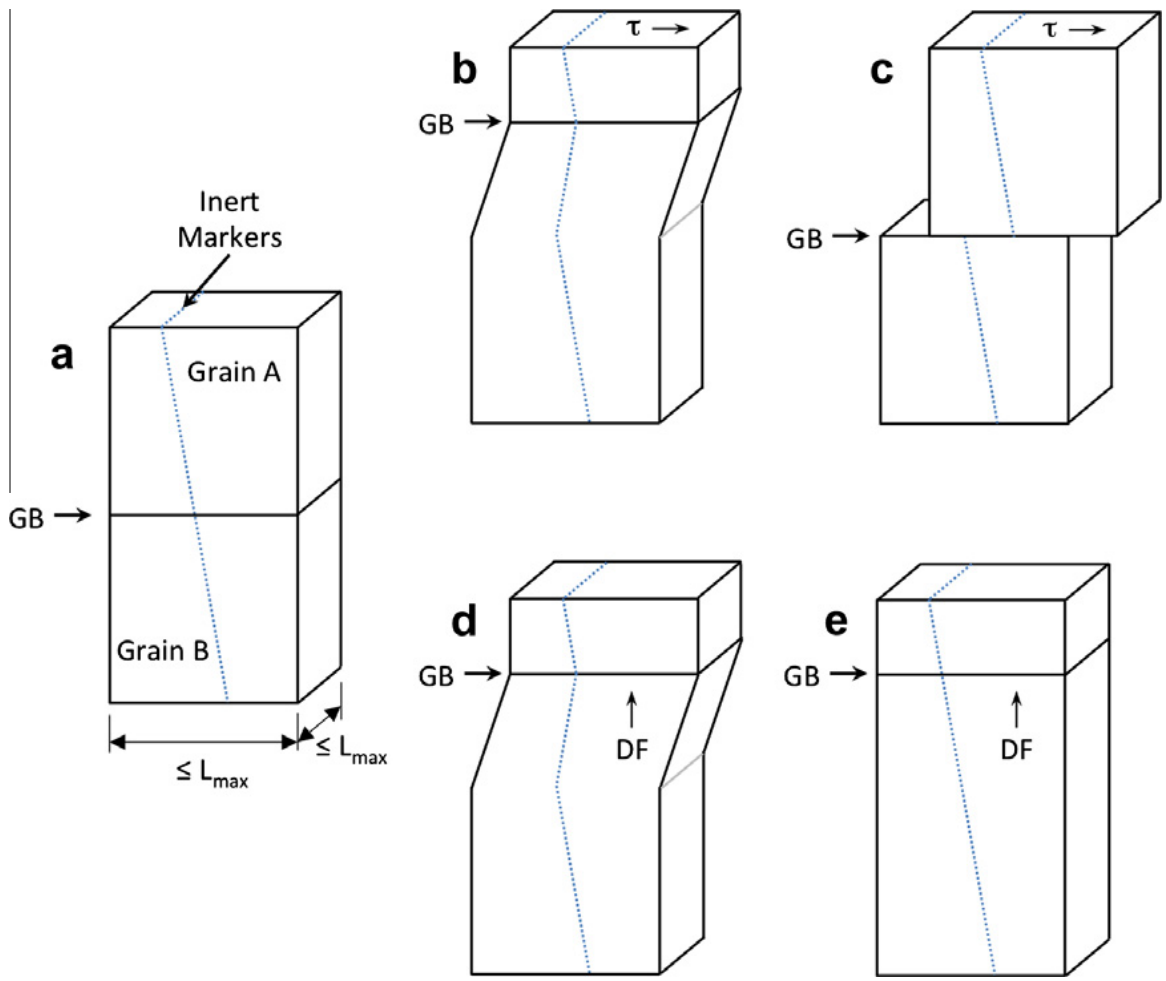

Figure 4.3. Illustration of the mechanical response of (a) a bicrystal with inert markers. Applied tractions can result in (b) shear-coupled migration of the boundary in the bicrystals or (c) sliding at the boundary with no boundary migration normal to the interface. A driving force applied normal to the boundary can result in (d) shear-coupled migration of the boundary in the bicrystals or (e) migration of the boundary normal to the interface without any lateral motion.

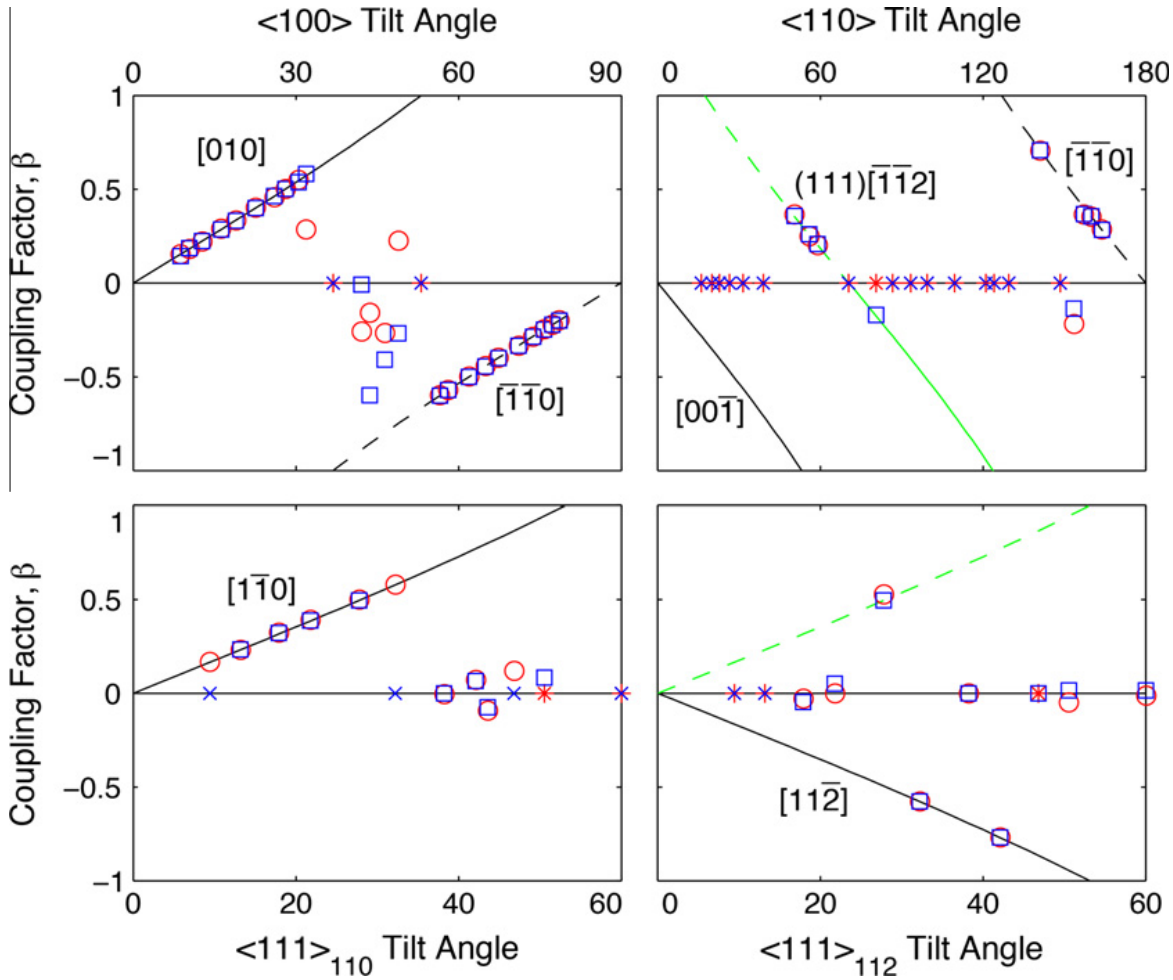

Figure 4.4. Shear coupling factors for the $\langle 100 \rangle$, $\langle 110 \rangle$, and $\langle 111 \rangle_{110}$ and $\langle 111 \rangle_{112}$ symmetric tilt boundaries as a function of the tilt angle at 1000 K. The theoretical coupling factors are plotted as solid and dashed lines, and are labeled according to the dislocation content. The $\langle 110 \rangle$ and $\langle 111 \rangle_{112}$ tilt boundaries have an addition coupling factor in green note suggested by the Frank-Bilby equation. The symbols represent simulation results. Boundaries that are immobile are denoted by xs.

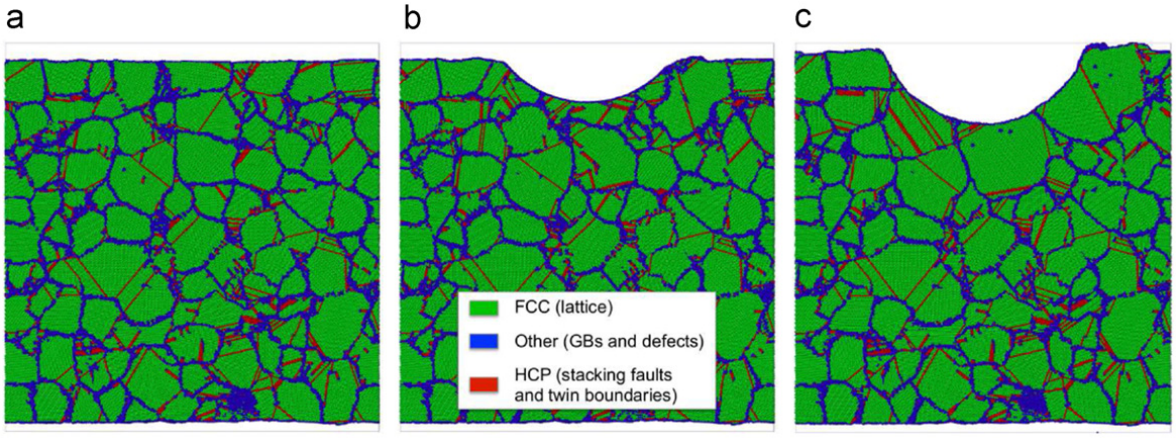

Figure 4.5. Snapshots showing the substructure evolution during surface indentation at (a) 0 ns, (b) 3 ns, and (c) 7.5 ns for an indentation rate of 1.0 m/s. Atoms are colored according to the computed common neighbor analysis (CNA) values (FCC = green, HCP = red and GBs = blue).

5. Precession Transmission Electron Microscopy

The results described in Chapter 2 clearly show the deposition and indentation conditions under which significant grain growth does and does not occur in nanocrystalline copper films. However, those data provide no indication or quantification of the characteristics of the nanocrystalline material, e.g. the evolution of texture and grain boundary character. The length scale associated with the material's nanocrystalline grains is inaccessible to conventional microstructure characterization techniques like electron backscatter diffraction, and so precession-enhanced electron diffraction in the transmission electron microscope was employed [18] to characterize the crystallographic texture, grain size, and grain-to-grain misorientation of the films before and after indentation.

Figure 5.1 shows the evolution of grain size in nanocrystalline, nanotwinned, $\langle 111 \rangle$-textured copper after indentation at cryogenic temperatures. The material in the pile-up around the indent shows appreciable grain growth (compare the green curve to the blue), supporting the results in Chapter 2. The heavily compressed material directly underneath the indenter shows mechanically-induced grain *refinement* due to the very large strains imparted to that region (compare the red curve to the blue).

Figure 5.2 shows the fraction of coincident site lattice (CSL) boundary types in untwinned and twinned nanocrystalline copper films after indentation. Since the data for the parent material in Fig 5.2(a) nominally corresponds to undeformed material, comparing Fig 5.2(a) with 5.2(b) provides insight into the evolution of CSL boundary character during / after indentation. The untwinned material (blue bars) exhibits no appreciable increase in the fraction of CSL boundaries as a result of indentation, and in fact perhaps shows a slight *decrease*. The nanotwinned material shows an obvious increase in CSL boundary content as a result of indentation, with the $\langle 100 \rangle$-textured film proliferating mostly $\Sigma 3$ boundaries and the $\langle 111 \rangle$-textured material generating $\Sigma 7$ content.

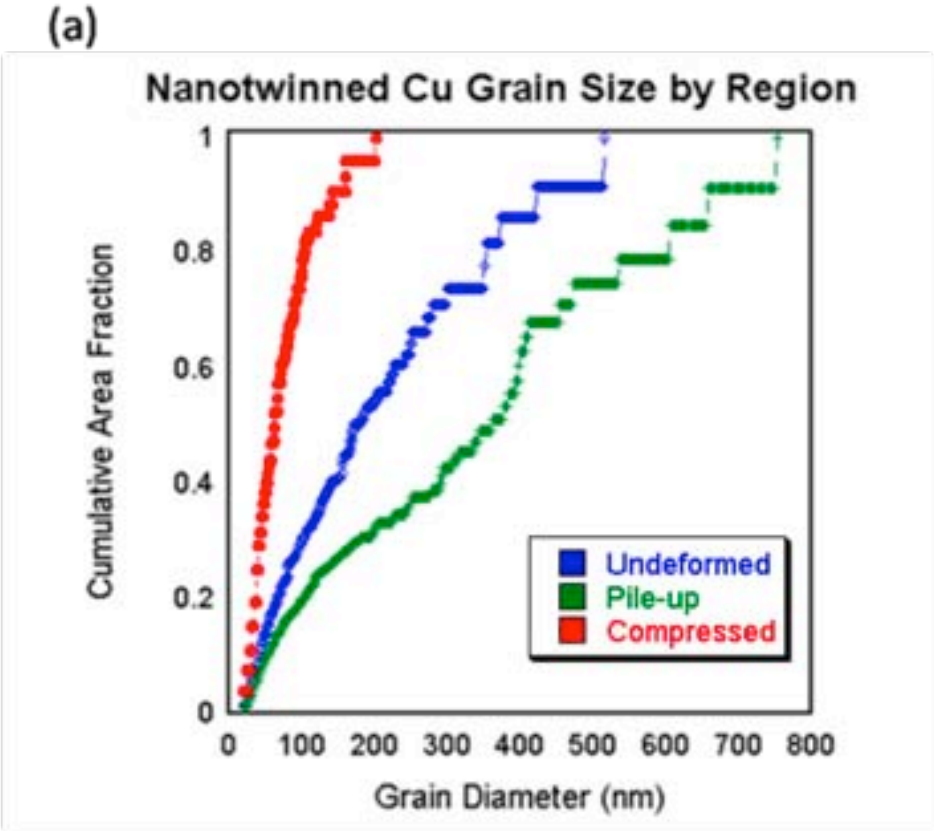

Figure 5.1. The evolution of grain size in nanocrystalline, nanotwinned copper after indentation at cryogenic temperatures.

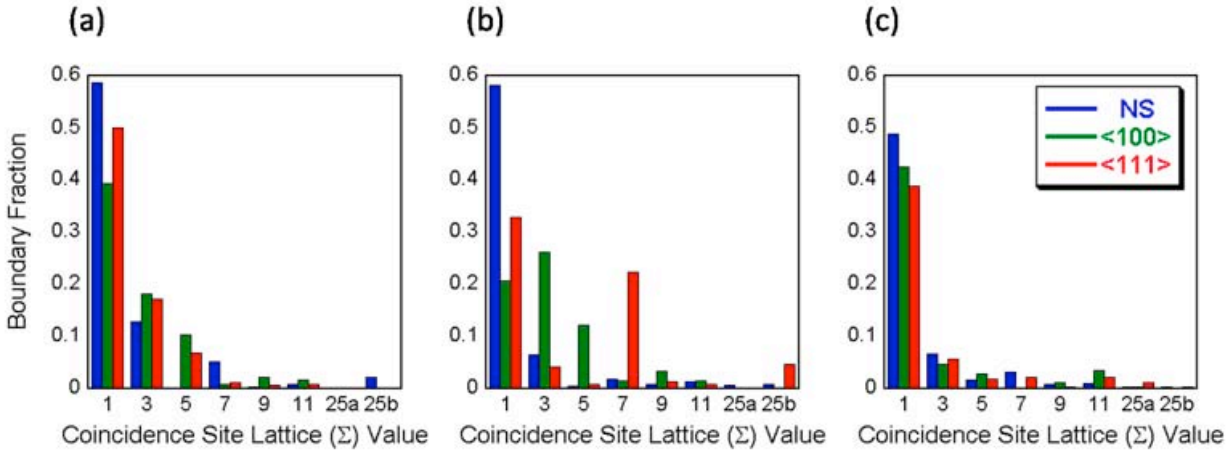

Figure 5.2. The fraction of coincident site lattice (CSL) boundary types in the (a) parent (undeormed), (b) pile-up (grain growth), and (c) indented (heavily deformed and grain refined) regions of nanocrystalline copper films. The blue bars correspond to untwinned material, and the green and red bars to ⟨100⟩- and ⟨111⟩-textured nanotwinned films, respectively.

6. *In-Situ* Cryogenic Indentation Experiments in the Transmission Electron Microscope

The findings outlined in the previous chapters provide important clues about the deposition and indentation conditions under which significant grain growth does and does not occur in nanocrystalline copper films, and about the types of grain boundaries that are important to this process. However, a number of open questions still remain. Among these is the ambiguity as to whether grain growth occurs during indentation while the films are cold, or after indentation once the films have warmed to room temperature. In the latter scenario, one could imagine that the inhibition of plasticity could lead to the development and storage of very large stresses during indentation, and these residual stresses promote grain growth after the samples are warmed. In an attempt to shed light on this issue, we developed a capability for performing cryogenic indentation inside a transmission electron microscope, so that the effects of indentation could be observed *in-situ* while the samples remained cold in a cryogenic environment. While this capability continues to evolve, this chapter outlines its early development and preliminary results therefrom.

To the best of the authors' knowledge, no commercial TEM stage has been developed for *in-situ* TEM cryogenic indentation, and no experiments of this type have been published in the open literature or attempted at other research facilities. As such, significant effort was placed into the design, development, and feasibility testing of such experiments. It was determined early that the cost and time associated with this effort could be significantly decreased by the use of a commercial *in-situ* TEM cryogenic straining stage operated in reverse. Sandia does not currently own such a stage. However, due to strong synergy with the microscopy team at Los Alamos, the authors were able to borrow a Gatan 671 single tilt liquid nitrogen cooled straining holder (Fig 6.1). Although the instrument permits real-time observation of the indentation process at cryogenic temperatures, it also has several limitations including a lack of precise positioning control, a non-standard loading geometry due to the wedge shapes of the indenter and sample, a requirement that the samples be electron transparent, and a limited control over heating and cooling rates. Despite these limitations, it was shown after several iterations that an *in-situ* TEM cryoidentaiton experiment is feasible with the sample and indenter design shown in Fig 6.1(b).

Capitalizing on the development of this new capability that permits us to perform *in-situ* TEM indentation experiments at cryogenic temperatures, this work has reproducibly investigated the microstructural evolution that occurs in nanocrystalline PLD copper during cryoindents. The lack of precise positioning control limits the study from having two elec-

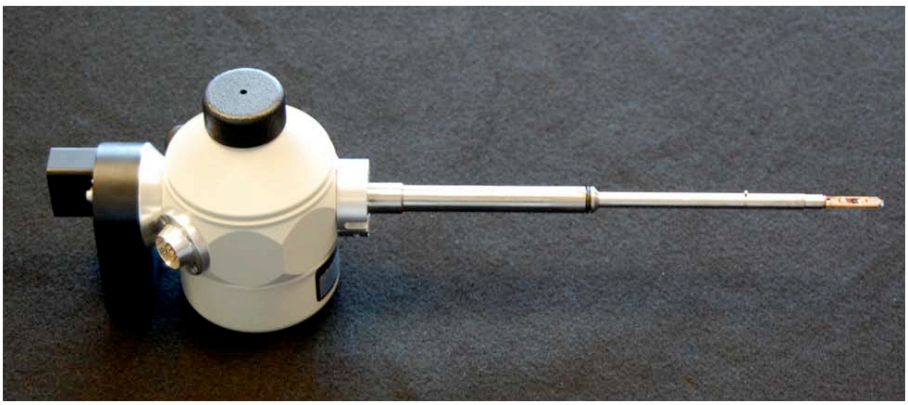

(a)

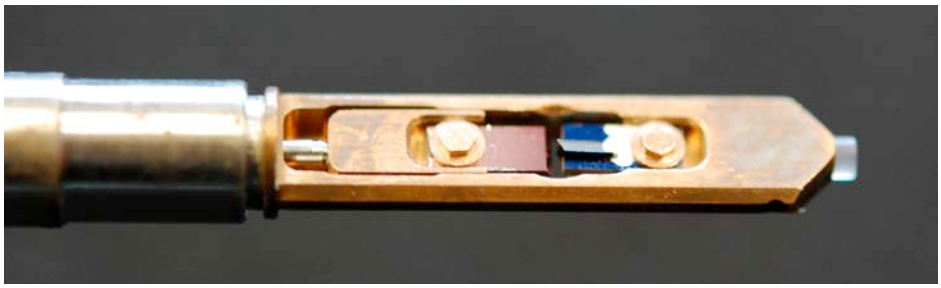

(b)

Figure 6.1. Images of (a) the *in-situ* TEM stage on loan from LANL and (b) the custom sample and indenter loaded into the stage.

tron transparent regions impinge on each other during the indentation. This means that the copper thin film can only be observed before and after indentation at high magnification, and not during. The indentation process itself can be observed at low magnification, as shown in Fig 6.2, wherein the careful approach of the indenter wedge onto the sample (Fig 6.2(a)) is followed by the deep penetration of the indenter wedge into the electron transparent copper film and silicon substrate. Any viewing angle in the mounting of the indenter wedge will shadow the indentation from being observed in the TEM. Despite this, the microstructure observed seconds after indentation can be characterized in the film after the indenter is withdrawn, as in Fig 6.2(c). Because the depth of the indentation and the two wedge structures involved, the stresses associated with these experiments could not be well characterized. In addition, it was often seen in these indents that material transfer could occur between the indenter tip and the film. The transfer from the indenter to the film was minimized by moving to harder coating necessary on the indenter tip to minimize charging effects. In Fig 6.2(c), some transfer of the copper film to the indenter is evident.

In addition to studying the microstructure of the nanocrystalline PLD copper film prior

(a) (b) (c)

Figure 6.2. Low magnification still frames taken (a) before, (b) during, and (c) after indentation of the custom wedge into a pulse laser deposition, nanotwinned copper film at cryogenic temperatures.

to and after indentation at cryogenic temperatures, this new capability also permits the study of the heating of the film from liquid nitrogen cryogenic temperatures to room temperature. The heating of the stage can be recorded through the thermocouple read-out developed with these experiments. It is suspected that the sample temperature and heating and cooling rates may vary from that of the recorded stage temperature due to the thermal drift observed. As such, the indentation was not performed until the sample had stabilized after cooling, and the final room temperature images were not taken until after the thermal drift had subsided. The microstructural evolution that occurs during the heating of the samples can be seen in Fig 6.3. At cryogenic temperatures after indentation, the nanocrystalline structure can still be observed in an area that is believed to be the pile-up of the film, Fig 6.3(a). As the sample heats up, some structural evolution can be observed in the transition between Fig 6.3(b) and Fig 6.3(c). This evolution can be associated with either minimal grain boundary motion or film bending. Care was taken to minimize the heating rate and thus the local bending, but this effect cannot be eliminated entirely, and it remain unclear as to its role in producing the behavior observed in Fig 6.3.

The results in Fig 6.3 do not show any obvious signs of abnormal grain growth in this preliminary experiment, either as a result of nanoindentation or as an effect of heating to room temperature. These results suggest that the grain growth observed during the *ex-situ* studies described in Chapter 2 were either a result of heating applied to a plastically deformed nanocrystalline region during sample preparation, or require a stress state that is not reproducible in our *in-sit*u TEM cryoindentation apparatus. Furthermore, while the results presented in this chapter are certainly preliminary, they hold great promise for future work to uncover key details and mechanisms behind the mysterious evolution of nanoycrystalline copper during / after cryogenic indentation. Additionally, it should be noted that, as aforementioned, to our knowledge these are the very first experiments of this type.

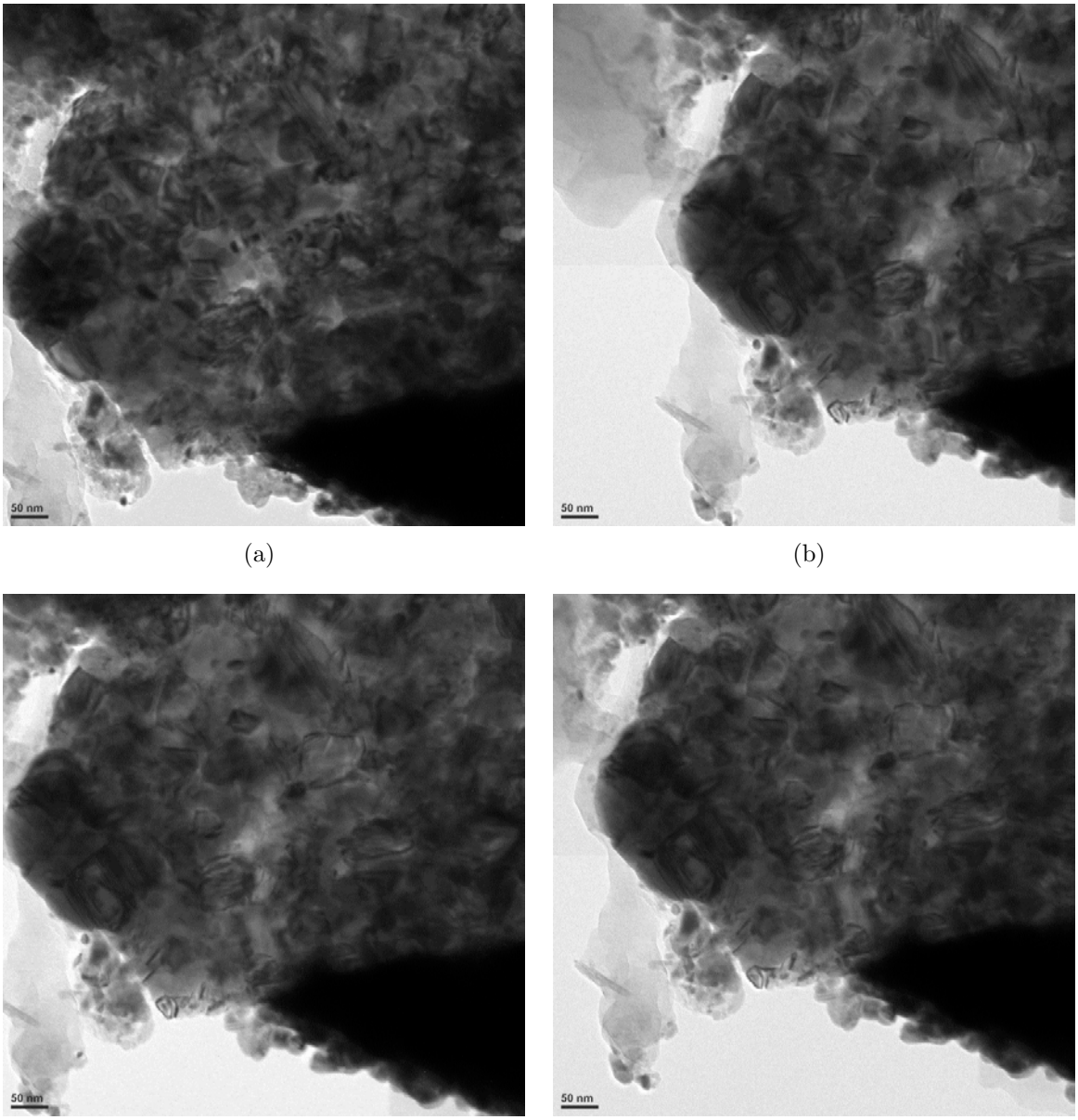

(a) (b) (c) (d)

Figure 6.3. A series of images taken during the warming of the pile-up region of the film during the warming from cryogenic temperatures to room temperature.

7. Conclusions

Visual inspection of scanning electron micrographs shows clear evidence of cryogenic grain growth in indented nanocrystalline copper films that contained nanotwins. Copper films that lacked twins were found to exhibit no substantial grain growth by visual inspection. Mesoscale simulations of grain growth accounting for both curvature and mechanical driving forces suggest that perhaps the suppression of plasticity at very low temperatures could lead to elevated stresses during indentation, which might manifest as driving forces that greatly exceed their ambient counterparts, and the dependence of this behavior on the presence of twins indicates their importance in governing the process. Precession transmission electron microscopy was used to confirm these findings quantitatively, and show that $\Sigma 3$ and $\Sigma 7$ boundaries proliferate during grain growth, implying that these interface types play a key role in governing the extensive grain growth observed here. These findings suggest a potential route toward grain boundary engineering as a means to mitigate the structural stability of nanocrystalline metals. Molecular dynamics simulations of the motion of individual grain boundaries demonstrate that specific classes of boundaries - notably $\Sigma 3$ and $\Sigma 7$ - exhibit anti- or a-thermal migration, meaning that their mobilities either *increase* or do not change significantly with *decreasing* temperature. However, none of these findings help to indicate whether grain growth in cryogenically indented, nanocrystalline, nanotwinned copper occurs at cryogenic temperatures, i.e. during or shortly after indentation, or whether it occurs after the samples have warmed to room temperature, perhaps due to the action of some elevated level of residual stress stored in the material during indentation. In an attempt to address this uncertainty, we developed a capability for in-situ cryogenic indentation of metal deposits in the transmission electron microscope. Although this effort proved exceedingly challenging and is still underway, preliminary results do not show the same level of extensive cryogenic grain growth observed in the miro-indentation experiments, either during indentation or after warming to room temperature. This discrepancy could arise from the significant differences in configuration and loading of the specimen between the two approaches, and further research and development of this capability is needed.

References

[1] J. A. Sharon, B. L. Boyce, Concepts on low temperature mechanical grain growth, in press SAND report (2013).

[2] K. Zhang, J. R. Weertman, J. A. Eastman, Rapid stress-driven grain coarsening in nanocrystalline cu at ambient and cryogenic temperatures, Applied Physics Letters 87 (6) (2005) 061921.

[3] J. G. Brons, H. A. Padilla II, G. B. Thompson, B. L. Boyce, Cryogenic indentation-induced grain growth in nanotwinned copper, Scripta Materialia 68 (10) (2013) 781.

[4] C. C. Battaile, W. A. Counts, G. W. Wellman, T. E. Buchheit, E. A. Holm, Simulating grain growth in a deformed polycrystal by coupled finite-element and microstructure evolution modeling, Metallurgical and Materials Transactions A 38A (1) (2013) 2513.

[5] E. R. Homer, E. A. Holm, S. M. Foiles, D. L. Olmsted, Non-thermally activated grain boundary motion and other new trends of grain boundary mobility, in preparation (2013).

[6] D. L. Olmsted, S. M. Foiles, E. A. Holm, Survey of computed grain boundary properties in face-centered cubic metals: I. grain boundary energy, Acta Materialia 57 (13) (2009) 3694.

[7] D. L. Olmsted, E. A. Holm, S. M. Foiles, Survey of computed grain boundary properties in face-centered cubic metals: Ii. grain boundary mobility, Acta Materialia 57 (13) (2009) 3704.

[8] A. P. Sutton, R. W. Balluffi, Interfaces in crystalline materials, Clarendon Press, Oxford, 1995.

[9] G. S. Rohrer, E. A. Holm, A. D. Rollett, S. M. Foiles, D. L. Olmsted, Comparing calculated and measured grain boundary energies in nickel, Acta Materialia 58 (15) (2010) 5063.

[10] E. A. Holm, G. S. Rohrer, S. M. Foiles, A. D. Rollett, H. M. Miller, D. L. Olmsted, Validating computed grain boundary energies in fcc metals using the grain boundary character distribution, Acta Materialia 59 (13) (2011) 5250.

[11] D. S. Gianola, S. van Petegem, M. Legros, S. Brandstetter, H. van Swygenhoven, K. J. Hemker, Stress-assisted discontinuous grain growth and its effect on the deformation behavior of nanocrystalline aluminum thin films, Acta Materialia 54 (8) (2006) 2253.

[12] T. J. Rupert, D. S. Gianola, Y. Gan, K. J. Hemker, Experimental observations of stress-driven grain boundary migration, Science 326 (5960) (2009) 1686.

[13] J. W. Cahn, Y. Mishin, A. Suzuki, Coupling grain boundary motion to shear deformation, Acta Materialia 54 (19) (2006) 4953.

[14] J. W. Cahn, Y. Mishin, A. Suzuki, Duality of dislocation content of grain boundaries, Philosophical Magazine 86 (25-26) (2006) 3965.

[15] E. R. Homer, S. M. Foiles, E. A. Holm, D. L. Olmsted, Phenomenology of shear-coupled grain boundary motion in symmetric tilt and general grain boundaries, Acta Materialia 61 (4) (2013) 1048.

[16] K. G. F. Janssens, D. L. Olmsted, E. A. Holm, S. M. Foiles, S. J. Plimpton, P. M. Derlet, Computing the mobility of grain boundaries, Nature Materials 5 (2) (2006) 124.

[17] G. J. Tucker, S. M. Foiles, Molecular dynamics simulations of rate-dependent grain growth during the surface indentation of nanocrystalline nickel, Materials Science and Engineering A 571 (2013) 207.

[18] J. G. Brons, H. A. Padilla II, K. A. Hattar, G. B. Thompson, B. L. Boyce, The role of copper twin boundaries in indentation-induced grain growth at 77 k, in preparation (2013).

DISTRIBUTION:

1	MS 1411	Amy C Sun, 01814
1	MS 1411	Paul G Clem, 01816
1	MS 0899	Technical Library, 9536 (electronic copy)
1	MS 0359	Donna L Chavez, LDRD Office, 1911

Sandia National Laboratories